

Matrix-filler interfaces and physical properties of metal matrix composites with negative thermal expansion manganese nitride

Koshi Takenaka, Kota Kuzuoka, and Norihiro Sugimoto

Citation: *Journal of Applied Physics* **118**, 084902 (2015); doi: 10.1063/1.4929363

View online: <http://dx.doi.org/10.1063/1.4929363>

View Table of Contents: <http://scitation.aip.org/content/aip/journal/jap/118/8?ver=pdfcov>

Published by the AIP Publishing

Articles you may be interested in

[Tailoring thermal expansion in metal matrix composites blended by antiperovskite manganese nitrides exhibiting giant negative thermal expansion](#)

J. Appl. Phys. **112**, 083517 (2012); 10.1063/1.4759121

[Effects of nitrogen deficiency on the magnetostructural properties of antiperovskite manganese nitrides](#)

J. Appl. Phys. **111**, 07E314 (2012); 10.1063/1.3672243

[The study of negative thermal expansion and magnetic evolution in antiperovskite compounds \$\text{Cu}_{0.8-x}\text{Sn}_x\text{Mn}_{0.2}\text{NMn}_3\$ \(\$0 \leq x \leq 0.3\$ \)](#)

J. Appl. Phys. **111**, 043905 (2012); 10.1063/1.3684653

[Giant negative thermal expansion in antiperovskite manganese nitrides](#)

J. Appl. Phys. **109**, 07E309 (2011); 10.1063/1.3540604

[Low-temperature negative thermal expansion of the antiperovskite manganese nitride \$\text{Mn}_3\text{CuN}\$ codoped with Ge and Si](#)

Appl. Phys. Lett. **93**, 081902 (2008); 10.1063/1.2970998




SHIMADZU
 Excellence in Science

Powerful, Multi-functional UV-Vis-NIR and FTIR Spectrophotometers

Providing the utmost in sensitivity, accuracy and resolution for applications in materials characterization and nano research

- Photovoltaics
- Polymers
- Thin films
- Paints
- Ceramics
- DNA film structures
- Coatings
- Packaging materials



Click here to learn more

Matrix-filler interfaces and physical properties of metal matrix composites with negative thermal expansion manganese nitride

Koshi Takenaka,^{1,2,a)} Kota Kuzuoka,¹ and Norihiro Sugimoto²

¹Department of Applied Physics, Nagoya University, Nagoya 464-8603, Japan

²Department of Crystalline Materials Science, Nagoya University, Nagoya 464-8603, Japan

(Received 7 June 2015; accepted 11 August 2015; published online 24 August 2015)

Copper matrix composites containing antiperovskite manganese nitrides with negative thermal expansion (NTE) were formed using pulsed electric current sintering. Energy dispersive X-ray spectroscopy revealed that the chemically reacted region extends over 10 μm around the matrix–filler interfaces. The small-size filler was chemically deteriorated during formation of composites and it lost the NTE property. Therefore, we produced the composites using only the nitride particles having diameter larger than 50 μm . The large-size filler effectively suppressed the thermal expansion of copper and improved the conductivity of the composites to the level of pure aluminum. The present composites, **having high thermal conductivity and low thermal expansion, are suitable for practical applications** such as a heat radiation substrate for semiconductor devices.

© 2015 AIP Publishing LLC. [<http://dx.doi.org/10.1063/1.4929363>]

I. INTRODUCTION

Thermal expansion is a ubiquitous phenomenon for solid materials. Although it is typically 10^{-5} to 10^{-6} in magnitude, even such a minute change fatally degrades the performance of devices and instruments in high-precision industries such as Ultra-Large Scale Integration (ULSI) fabrication. Furthermore, **for a device comprising multiple materials, mismatch in thermal expansion between the constituents themselves causes severe damage** such as exfoliation of interfaces and breakage of wires. Consequently, strong demand exists for a means to adjust thermal expansion of a material to some particular value, typically zero, in many fields of engineering, including machining and processing, optics, and electronics. Furthermore, for green technologies such as fuel cells and thermoelectric converters, control of thermal expansion in joints is a key issue for high performance and longevity.

For the control of thermal expansion in materials, composites of various types filled with materials that contract on heating, or negative thermal expansion (NTE) materials,^{1–5} have been designed to date. However, it is difficult to say that NTE materials known to date such as β -eucryptite ($\text{LiAlSi}_4\text{O}_{12}$) and ZrW_2O_8 have sufficient thermal expansion restraint capability. **In the field of NTE research, remarkable development has been achieved over the last decade.** Particularly, after the discovery of gigantic NTE in antiperovskite manganese nitrides Mn_3AN (A: metal or semiconducting element),^{6–11} many giant NTE materials were discovered successively: $\text{SrCu}_3\text{Fe}_4\text{O}_{12}$,¹² $\text{Bi}_{1-x}\text{Ln}_x\text{NiO}_3$ (Ln: lanthanoid),^{13,14} $\text{La}(\text{Fe}, \text{Si}, \text{Co})_{13}$,¹⁵ $\text{MnCo}_{0.98}\text{Cr}_{0.02}\text{Ge}$,¹⁶ and others.

The NTE of the recently discovered materials well exceeds -30 ppm K^{-1} in α , coefficient of linear thermal expansion, with materials reaching -100 ppm K^{-1} among

them. Several attempts to form polymer matrix composites (PMCs) containing these giant NTE materials have been successful, demonstrating that large thermal expansion of polymers can be reduced to almost zero.^{17,18} Regarding metal matrix composites (MMCs), however, few reports have described studies of manganese nitrides^{19–21} because these giant NTE materials have high chemical reactivity with molten metals. Pulsed electric current sintering reduces both the temperature and time for fabrication of MMCs, thereby enabling the use of metals of various kinds including Al, Cu, and Ti as a matrix.²⁰ The giant NTE of the manganese nitrides controlled the overall thermal expansion of the MMCs across widely various α values, including even negative ones. However, quantitative analysis based on theoretical models suggests that the suppression of thermal expansion is not as great as expected. Chemical and physical investigations of the matrix-filler interfaces must be undertaken for better composite performance.

This report describes a study of copper matrix composites with void-free NTE manganese nitride filler. The void-free grains were obtained by crushing the densely sintered body of the pure manganese nitride. The present analysis revealed that the chemically reacted region extends over 10 μm around the interfaces. The small nitride grains are ineffective for the suppression of thermal expansion because these small particles lose their NTE performance during formation of composites. Then, we sifted the crushed manganese nitrides and sorted out only those particles having diameter larger than 50 μm . Consequently, the obtained large-size filler exhibits much higher capability of thermal-expansion compensation and improves the conductivity of the composites.

II. EXPERIMENTAL

The thermal-expansion compensator, antiperovskite manganese nitride $\text{Mn}_{2.95}\text{Cu}_{0.1}\text{Zn}_{0.55}\text{Sn}_{0.4}\text{N}$, was prepared

^{a)}Author to whom correspondence should be addressed. Electronic mail: takenaka@nuap.nagoya-u.ac.jp

using solid-state reactions with powders of Mn_2N and pure elements Cu, Zn, and Sn (purity, 99.9%; particle size, 30–50 μm).^{20,22,23} The obtained nitride was roughly pulverized in an agate mortar. We mixed this nitride and copper powders (purity, 99.99%; particle size, $\sim 1 \mu\text{m}$) in a volume ratio of 25:75, packed them in a graphite die, and installed it in a spark plasma sintering (SPS) furnace (Syntex Lab; SPS Syntex Inc.). Sintering was conducted under pressure of 100 MPa at 475 °C for 7 min in a vacuum ($<10^{-1}$ Pa). Composites of this type are called “as-grown-filler” composite herein. We also made composites of three other types, which contain the void-free manganese nitride filler. To obtain dense ceramic filler, the as-grown manganese nitride was pulverized down to 8–12 μm diameter, packed in a graphite die, and sintered using the SPS furnace under pressure of 100 MPa at 650 °C for 10 min in the vacuum. Density of the sintered nitride was determined to be 98% or higher using Archimedes’ method. The obtained sintered body was crushed and sifted using a 53 μm -mesh sieve. It was divided into three kinds by particle size: as-crushed (without sieving), 102- μm median diameter (not passed through the sieve), and 14- μm median diameter (passed through the sieve). The median diameter was ascertained using a laser diffraction/dispersion-type particle diameter analyzer (LA-950V2; Horiba). The copper matrix composites containing void-free fillers of the above three types were formed in the same manner as the as-grown-filler composite. Composites of these types are designated, respectively, as “void-free/as-crushed-filler,” “void-free/102- μm median diameter filler,” and “void-free/14- μm median diameter filler” composites.

The sample surfaces were observed using a digital microscope (VHX-1000; Keyence) and by a scanning electron microscope (SEM, VE-7800; Keyence). To verify the chemical reaction between the metal matrix and the

thermal-expansion compensator, we analyzed the chemical composition of the interface region of the MMCs using energy dispersive X-ray spectroscopy (EDX, Genesis 2000K; EDAX Inc.). The chemical identification and the crystal structure analysis were conducted at room temperature T using X-ray powder diffraction (XRD, RINT2000; Rigaku). Linear thermal expansion $\Delta L(T)/L$ was measured using a laser-interference dilatometer (LIX-2; Ulvac). Temperature dependence of electrical resistivity $\rho(T)$ was measured using a conventional four-probe technique.

III. RESULTS

Figure 1(a) portrays a microscopic image of 25 vol. %- $\text{Mn}_{2.95}\text{Cu}_{0.1}\text{Zn}_{0.55}\text{Sn}_{0.4}\text{N}/\text{Cu}$ composite with the *as-grown filler*. The microscopic observation indicates almost even distribution of the matrix and the filler, but the composites seem to include a certain amount of voids. These voids exist inside the filler rather than in interfaces between the matrix and the filler because the as-grown filler consists of the loosely aggregated nitride grains. These voids must be removed because they can degrade physical properties of the composites.

Next, we show microscopic images of 25 vol. %- $\text{Mn}_{2.95}\text{Cu}_{0.1}\text{Zn}_{0.55}\text{Sn}_{0.4}\text{N}/\text{Cu}$ composites with the *void-free filler*. Figures 1(b), 1(c), and 1(d), respectively, depict images of the composites containing the void-free/as-crushed, the void-free/102- μm median diameter, and the void-free/14- μm median diameter fillers. These photographs clearly portray that the voids are reduced markedly in comparison with the as-grown-filler composite shown in Fig. 1(a). We also confirm almost even distribution of the matrix and the filler.

Then, we evaluated how chemical reactions progressed between the matrix and the filler when forming composites.

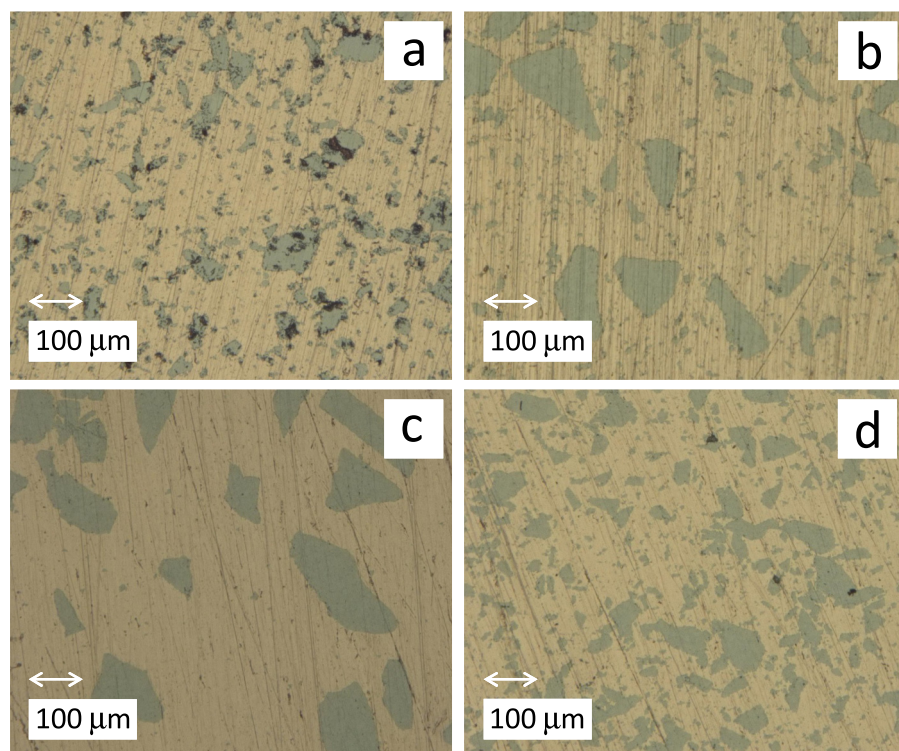


FIG. 1. Microscopic image of 25 vol. %- $\text{Mn}_{2.95}\text{Cu}_{0.1}\text{Zn}_{0.55}\text{Sn}_{0.4}\text{N}/\text{Cu}$ composites: (a) as-grown, (b) void-free/as-crushed, (c) void-free/102- μm median diameter, (d) and void-free/14- μm median diameter fillers.

TABLE I. Averaged molar fraction of elements for the Cu matrix and the nitride filler by energy dispersive X-ray analysis (unit: %).

	Cu	Mn	Zn	Sn
Cu matrix	98.26	0.53	0.78	0.43
Nitride filler	2.24	73.27	14.61	9.88

The XRD profile after sintering is a superimposition of the individual patterns of the matrix and the filler (see, Ref. 20). We used SEM-EDX to evaluate the chemical compositions around the interface region. In the present analysis, we did not consider the contents of nitrogen because SEM-EDX cannot provide reliable information about light elements such as nitrogen. Table I presents results for the Cu matrix and the void-free manganese nitride themselves. The results on the inside and outside of a 100- μm nitride grain in the composites with the void-free/102- μm median diameter filler are shown, respectively, in Tables II and III. The results on the 10- μm nitride grain in the composites with the void-free/102- μm median diameter filler are shown, respectively, in Tables IV and V. The small size particles less than 53 μm are not perfectly removed from the 102- μm median diameter filler. Indeed, we recognize the small size particles in Fig. 1(c). The SEM images of the above samples are presented in Fig. 2. The molar fraction of Cu and Mn elements inside and outside of the nitride grains is shown in Fig. 3. The arrow in Fig. 2 shows the analysis points. The series of analyses suggest that chemical reactions progressed about 10 μm in the interfacial region.²⁴ In other words, as for the small grains about 10 μm in diameter, the whole grain chemically reacted exhaustively with the matrix and is regarded as lose its ability as a thermal-expansion compensator. The result presented above implies that choosing only large nitride grains as the filler might improve the composite performance. This expectation was supported by the following experiments.

Figure 4(a) portrays the linear thermal expansion $\Delta L/L$ for the composites of above four types. For comparison, $\Delta L/L$ of the filler and the matrix themselves are also shown.

TABLE II. Molar fraction of elements for the 100- μm nitride grain in the Cu matrix composite with the void-free/102- μm median diameter filler (unit: %). See Figs. 2(a) and 3(a).

Distance (μm)	Cu	Mn	Zn	Sn
0	40.35	43.71	9.89	6.04
1	17.07	61.59	13.06	8.28
2	9.47	68.31	12.80	9.43
3	7.43	70.08	13.71	8.78
4	7.03	70.52	13.40	9.05
5	6.27	70.69	14.11	8.94
6	5.85	71.04	13.85	9.26
7	4.91	72.01	14.24	8.85
8	4.44	70.91	14.05	10.60
9	4.36	71.89	13.90	9.86
10	3.30	71.32	14.97	10.41
11	2.80	76.93	12.76	7.51
12	2.60	73.47	14.65	9.28
20	2.99	73.89	13.83	9.28
Center	2.52	73.38	14.40	9.69

TABLE III. Molar fraction of elements for the Cu matrix outside the 100- μm nitride grain in the composite with the void-free/102- μm median diameter filler (unit: %). See Figs. 2(a) and 3(a).

Distance (μm)	Cu	Mn	Zn	Sn
1	77.25	17.31	2.89	2.55
2	87.35	7.66	3.40	1.59
3	90.61	5.46	2.85	1.08
4	91.74	3.63	3.60	1.04
5	94.14	3.43	1.26	1.17
10	95.13	2.27	1.62	0.98
20	96.29	1.76	0.76	1.19

The nitride filler $\text{Mn}_{2.95}\text{Cu}_{0.1}\text{Zn}_{0.55}\text{Sn}_{0.4}\text{N}$ exhibits NTE of $\alpha = -34 \text{ ppm K}^{-1}$ at $T = 330\text{--}365 \text{ K}$ (operating-temperature window $\Delta T = 35 \text{ K}$), which reduces the thermal expansion of the composites. The α values at 350 K are -0.8 ppm K^{-1} (void-free/102- μm median diameter filler), 2.3 ppm K^{-1} (void-free/as-crushed filler), 3.2 ppm K^{-1} (as-grown filler), and 4.9 ppm K^{-1} (void-free/14- μm median diameter filler). This sequence of the α values supports the inference that the ability to reduce thermal expansion becomes higher as the filler grain size increases. Particularly, the void-free/14- μm median diameter filler is inferior to the void-contained, as-grown filler. The present result presents the severe effects of chemical deterioration for small-size filler.

Figure 5 shows the electrical resistivity $\rho(T)$ for the composites of four types. The overall resistivity of the composites is metallic ($d\rho/dT > 0$) because both the matrix and the filler are metallic.^{25–27} The resistivity increases in the sequence of the void-free/102- μm median diameter filler, as-grown filler, void-free/as-crushed filler, and void-free/14- μm median diameter filler. The dispersion in data is much greater for the composites containing the as-grown and the as-crushed fillers than composites of the other two types. Therefore, the difference in ρ data suggested for the as-grown and the as-crushed filler composites might not be physically significant. This is true partly because the filler grain size was not controlled for composites of these two types. Consequently, the dispersion in the grain size was large among the samples prepared for the ρ measurements. The composite containing the void-free/102- μm median diameter filler shows the lowest resistivity, $3.9 \mu\Omega \text{ cm}$ at 300 K. Assuming the Wiedemann–Franz law, it corresponds

TABLE IV. Molar fraction of elements for the 10- μm nitride grain in the Cu matrix composite with the void-free/102- μm median diameter filler (unit: %). See Figs. 2(b) and 3(b).

Distance (μm)	Cu	Mn	Zn	Sn
1	33.24	50.01	10.18	6.57
2	13.18	67.03	11.92	7.87
3	9.79	69.79	12.64	7.78
4	8.56	69.37	14.91	7.15
5	8.06	69.48	13.32	9.14
6	8.62	67.32	13.62	10.44
7	9.08	66.89	13.25	10.76
8	28.25	52.63	10.66	8.47

TABLE V. Molar fraction of elements for the Cu matrix outside the 10- μm nitride grain in the composite with the void-free/102- μm median diameter filler (unit: %). See Figs. 2(b) and 3(b).

Distance (μm)	Cu	Mn	Zn	Sn
1	80.85	11.95	4.46	2.74
2	90.25	5.18	3.27	1.30
3	93.58	3.84	2.03	0.55
4	94.71	2.48	1.98	0.83
5	94.88	1.94	2.42	0.76
6	95.98	1.32	1.46	1.24
7	95.70	1.49	2.13	0.69
8	95.17	1.91	1.82	1.10
9	96.80	1.11	1.64	0.45
10	97.75	1.09	0.01	1.16

to the thermal conductivity of $190 \text{ W m}^{-1} \text{ K}^{-1}$, which is as high as that of pure aluminum ($200 \text{ W m}^{-1} \text{ K}^{-1}$). The preliminary measurement by a laser-flash technique suggests that thermal conductivity at room temperature is about $200 \text{ W m}^{-1} \text{ K}^{-1}$ for the composite with the void-free/102- μm median diameter filler, which is consistent with the present estimate based on the Wiedemann-Franz law. Note that the residual resistivity of the composite with the

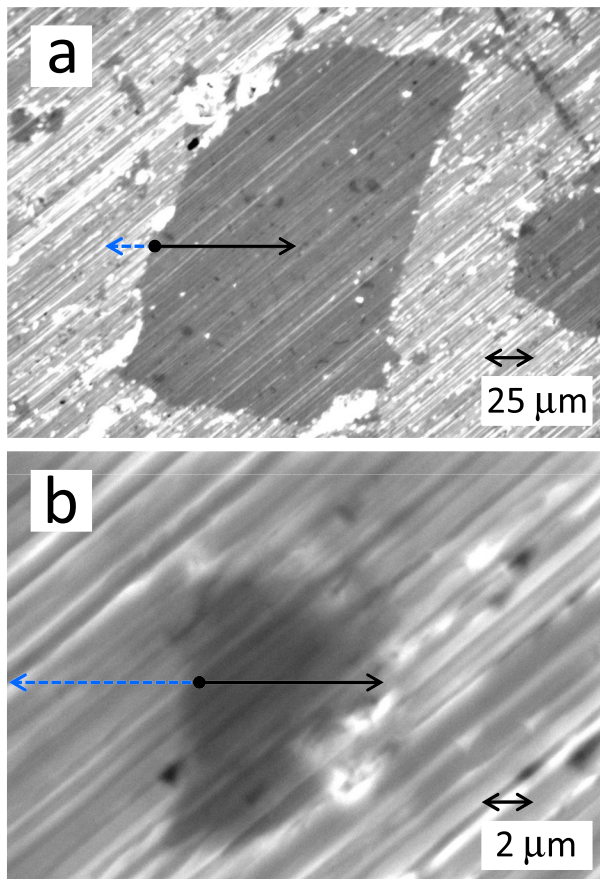


FIG. 2. SEM images of the nitride grains in 25 vol. %- $\text{Mn}_{2.95}\text{Cu}_{0.1}\text{Zn}_{0.55}\text{Sn}_{0.4}\text{N}$ /Cu composite with the void-free/102- μm median diameter filler: (a) 100 μm and (b) 10 μm grains. Solid and dashed arrows, respectively, indicate the distances of the EDX-analysis points inside and outside of the grain, as shown in Tables II–IV. Solid circles correspond to the 0 μm points.

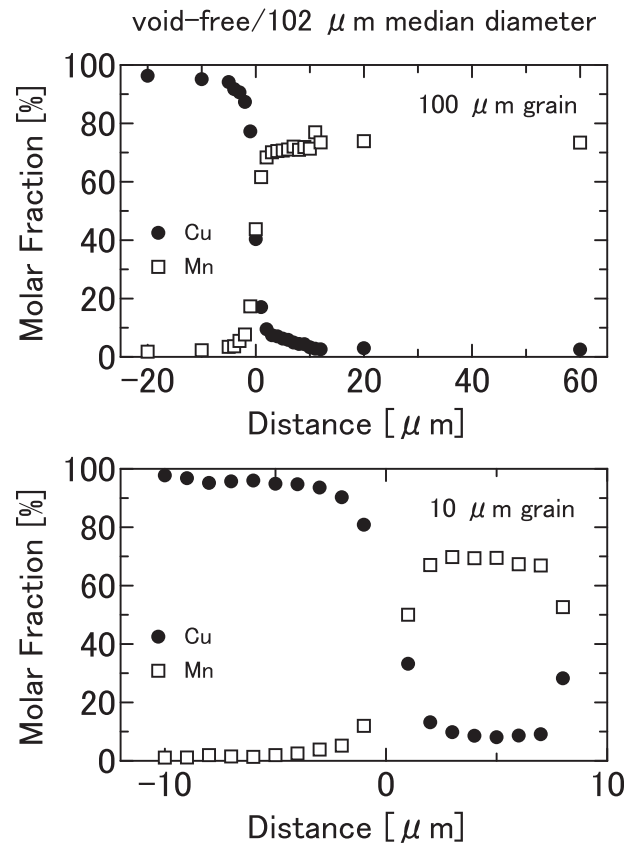


FIG. 3. Molar fraction of Cu and Mn elements inside and outside of the 100- μm (a) and 10- μm (b) nitride grains in 25 vol. %- $\text{Mn}_{2.95}\text{Cu}_{0.1}\text{Zn}_{0.55}\text{Sn}_{0.4}\text{N}$ /Cu composite with the void-free/102- μm median diameter filler. The SEM images and the results of SEM-EDX analyses are shown in Fig. 2 and in Tables II–IV, respectively.

void-free/14- μm median diameter filler is extremely high, which is later discussed.

IV. DISCUSSION

The obtained thermal expansion of the composites was analyzed using two theoretical bounds, rule of mixture (ROM) and Turner's models, in which particles of an isotropic thermal-expansion-compensating filler are uniformly dispersed in an isotropic matrix.^{3,28} The former bound is given by assuming that thermally induced *stress* is uniform everywhere throughout a composite, which is equivalent to the assumption that the matrix and the thermal-expansion compensator exhibit their own thermal expansion independently. Consequently, the thermal expansion of a composite is given by the volume-weighted sum of the contributions from the matrix and the dispersed filler.

$$\alpha_c = v_m \alpha_m + v_f \alpha_f. \quad (1)$$

Here, subscripts c, m, and f, respectively, denote the composite, matrix, and filler. v_m and v_f are the volume fractions of the matrix and the filler, respectively, and $v_m + v_f = 1$.

The latter bound is given by the approximation that thermally induced *strain* is uniform throughout a composite, as proposed first by Turner:

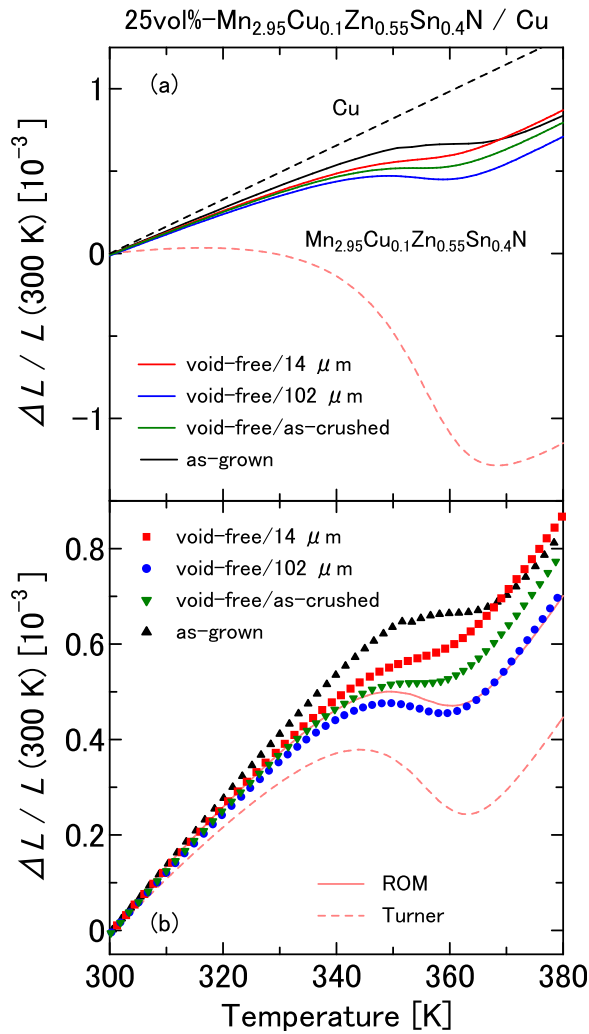


FIG. 4. (a) Linear thermal expansion of 25 vol. % $\text{Mn}_{2.95}\text{Cu}_{0.1}\text{Zn}_{0.55}\text{Sn}_{0.4}\text{N} / \text{Cu}$ composites: as-grown (black), void-free/as-crushed (green), void-free/102- μm median diameter (blue), and void-free/14- μm median diameter (red) fillers. Linear thermal expansion of pure copper and $\text{Mn}_{2.95}\text{Cu}_{0.1}\text{Zn}_{0.55}\text{Sn}_{0.4}\text{N}$ is also shown. (b) Experimental plots of linear thermal expansion and curves calculated using ROM and Turner's model for 25 vol. % $\text{Mn}_{2.95}\text{Cu}_{0.1}\text{Zn}_{0.55}\text{Sn}_{0.4}\text{N} / \text{Cu}$ composites.

$$\alpha_c = \frac{v_m E_m \alpha_m + v_f E_f \alpha_f}{v_m E_m + v_f E_f}. \quad (2)$$

Here, E is the Young's modulus. In Eq. (2), the element with the larger elastic modulus contributes more to the thermal expansion of the composite. In the present analysis, E_m and E_f are assumed to be 125 GPa²⁹ and 200 GPa,³⁰ respectively, and $\alpha_m > \alpha_f$ is satisfied in the displayed T region. Therefore, Eq. (1) gives the upper bound and Eq. (2) gives the lower bound for α_c . In the case of the MMCs, E_m and E_f are not so different as the PMCs. Therefore, these two bounds are not so different as the PMCs.¹⁷ In the following, thermal expansion of the composites is evaluated also based on $\Delta L(T)/L$ (integral of α) in addition to α because α of these composites changes drastically around the operating temperature of NTE.

Figure 4(b) displays a plot of the $\Delta L(T)/L$ experimental values and curves calculated assuming ROM and Turner's moles for the 25 vol. % $\text{Mn}_{2.95}\text{Cu}_{0.1}\text{Zn}_{0.55}\text{Sn}_{0.4}\text{N} / \text{Cu}$

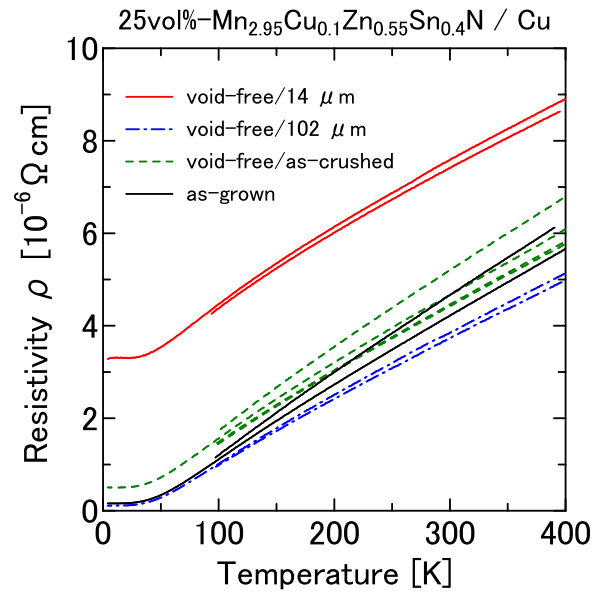


FIG. 5. Temperature-dependent resistivity of 25 vol. % $\text{Mn}_{2.95}\text{Cu}_{0.1}\text{Zn}_{0.55}\text{Sn}_{0.4}\text{N} / \text{Cu}$ composites: as-grown (black), void-free/as-crushed (green), void-free/102- μm median diameter (blue), and void-free/14- μm median diameter (red) fillers.

composites. It is noteworthy that the $\Delta L(T)/L$ for the void-free/102- μm median diameter filler composite is in between the ROM and the Turner's models, although $\Delta L(T)/L$ for others are even larger than the theoretical upper limit ROM. For MMCs containing the NTE nitrides, the thermal expansion below the volume-weighted sum (ROM estimation) has not been reported to date except the MMCs formed by pressure infiltration.³ In most cases, the obtained thermal expansion is at smallest comparable with the ROM estimation. For the Ti matrix composites, the thermal expansion is larger than the upper limit ROM.²⁰ The present result demonstrates that reduction of the interface-to-volume ratio is effective for suppressing thermal expansion of the MMCs.

Next, we examine what is formed at interfaces by chemical reactions between the matrix and the filler. Extremely high residual resistivity of the void-free/14- μm median diameter filler composite, in which the ratio of the interface to the volume is the highest, suggests low crystallinity of the reacted materials. Some amorphous materials might be formed at interfaces because we do not recognize a XRD pattern suggesting the third materials other than the matrix and the filler. The present SEM-EDX analysis provides us with information related to compositional ratio of the elements only. Identification of the materials has yet to be explored. The remarkable grain-size dependence of thermal expansion suggests an interface imperfection such as discontinuities of stress and/or displacement across it.³¹ However, the interfacial chemical reaction is not only associated with negative effects. The interfacial material might increase the adhesion of the matrix and the filler overcoming large discrepancy in their α values. It will manifest itself as enhancement of the mechanical strength of the composites.

Increase in density of the nitride filler itself is expected not only to reduce voids from the composites and to suppress excess interfacial chemical reactions but also to improve the

transport properties. The improvement of the conductivity thus obtained might not be ascribed only to suppression of the interface-to-volume ratio. The transport properties of the manganese nitrides depend strongly on the degree of sintering. Electrical resistivity was reported as 2–3 m Ω cm in the early stage of research,²⁵ but the reported values decrease to 200–300 $\mu\Omega$ cm with improvement of sintering.^{26,27} Compared with electrical resistivity, thermal conductivity κ is little reported. According to the study of Huang *et al.*,³² thermal conductivity of the NTE manganese nitrides is typically 3.6 W m⁻¹ K⁻¹ at room temperature. Assuming the Wiedemann–Franz law, it corresponds to electrical resistivity of 200 $\mu\Omega$ cm. In real materials, phonon also contributes to thermal conductance. Therefore, 3.6 W m⁻¹ K⁻¹ might be physically too small. It is partly explained by low degree of sintering. Much void was included in the nitride filler grains used for the past.²⁰ Therefore, the conductivity of the filler itself is regarded as suppressed.

The NTE manganese nitrides present several advantages over other NTE materials, such as large, isotropic, and rigid NTE.³⁰ Therefore, the manganese nitrides can suppress thermal expansion of a metal effectively, although a metal has higher rigidity and therefore induces greater inner stress at interfaces than polymers. Although an operating-temperature window is limited, the MMCs operate over several tens of degrees, which is sufficiently wide for precise devices and instruments designated for room-temperature operation. In such an important T region, the manganese nitrides can suppress thermal expansion of a metal down to even negative α by only 25 vol. % filler loading. In many cases, it is difficult for other NTE materials to achieve negative α in a MMC.^{33,34} Even for ZrW₂O₈/Al³⁵ and ZrW₂O₈/Cu³⁶ composites, α became almost zero or even slightly negative for the 75 vol. % filler loading. Another example of negative α is a case of the Sc₂W₃O₁₂-core/Cu-shell composite, in which the volume fraction of Sc₂W₃O₁₂ showing NTE is extremely high: over 80 vol. %.³⁷ Finely tuned negative α in the present composites enables us, for example, to athermalize a fiber Bragg grating.³⁸

One of possible applications of the present MMCs is heat sink materials for power devices. For this purpose, high thermal conductivity comparable with that of pure Al ($\kappa \sim 200$ W m⁻¹ K⁻¹) and low thermal expansion comparable with SiC ($\alpha \sim 5$ ppm K⁻¹) are necessary. We have no single-component metal materials meeting such difficult criteria, but present MMCs might satisfy this condition (Table VI). The nitride filler used here shows rather large negative α with the narrow T window ($\Delta T \sim 35$ K). Therefore, α of the composite becomes even negative at smallest, but thermal expansion does not show T -linear dependence, and total expansion $\Delta V/V$ at the important T interval (320–380 K) is slightly larger than required value. The composite performance can be upgraded by further improvement of the interfaces. The better interfaces make the elastic interaction between the matrix and the filler more effective, which will bring the composite thermal expansion close to the Turner's estimation. The better interfaces can also improve thermal conductivity. Because the achieved thermal conductivity is greatly less than the ROM estimation

TABLE VI. Comparison between the physical properties required for the heat sink materials and the specific values achieved by the 25 vol. %-Mn_{2.95}Cu_{0.1}Zn_{0.55}Sn_{0.4}N/Cu composite with the void-free/102- μ m median diameter filler.

	α (ppm K ⁻¹) (350 K)	$\Delta V/V$ (10 ⁻³) (320–380 K)	κ (W m ⁻¹ K ⁻¹) (300 K)
Required values	5	1.20	>200
Achieved values	-0.8	1.36	190 ^a

^a κ of the composite is estimated from the measured electrical resistivity (3.9 $\mu\Omega$ cm) via Wiedemann–Franz law.

($\kappa_{\text{ROM}} = v_m \kappa_m + v_f \kappa_f \sim 0.75 \times 400 + 0.25 \times 3.6 \sim 300$ W m⁻¹ K⁻¹), there is plenty of room for improvement.

V. CONCLUSION

Sintering processes used for forming composite cause chemical reactions between the copper matrix and the nitride filler over 10 μ m around the interfaces. Therefore, small nitride grains having a radius of about 10 μ m or less do not contribute to the suppression of thermal expansion. We produced the composites using only nitride grains having diameter greater than 50 μ m, which were obtained by crushing the densely sintered body. The large-size filler can produce composites with high conductivity and low thermal expansion, which are suitable for applications such as heat-sink materials.

ACKNOWLEDGMENTS

The authors are grateful to Y. Okamoto for his helpful comments. They also thank T. Hamada and K. Otsuka for their assistance with the experiments. This work was supported in part by the Ministry of Education, Culture, Sports, Science and Technology of Japan (Grant Nos. 22360291 and 26108709), by NEDO, Japan (Grant No. 08A19009d), by the Asahi Glass Foundation, and by the Toyota Physical and Chemical Research Institute.

¹A. W. Sleight, *Inorg. Chem.* **37**, 2854 (1998).

²W. Miller, C. W. Smith, D. S. Mackenzie, and K. E. Evans, *J. Mater. Sci.* **44**, 5441 (2009).

³K. Takenaka, *Sci. Technol. Adv. Mater.* **13**, 013001 (2012).

⁴C. Lind, *Materials* **5**, 1125 (2012).

⁵J. Chen, L. Hu, J. X. Deng, and X. R. Xing, *Chem. Soc. Rev.* **44**, 3522 (2015).

⁶K. Takenaka and H. Takagi, *Appl. Phys. Lett.* **87**, 261902 (2005).

⁷R. J. Huang, L. F. Li, F. S. Cai, X. D. Xu, and L. H. Qian, *Appl. Phys. Lett.* **93**, 081902 (2008).

⁸Z. H. Sun, X. Y. Song, F. X. Yin, L. X. Sun, X. K. Yuan, and X. M. Liu, *J. Phys. D: Appl. Phys.* **42**, 122004 (2009).

⁹J. C. Lin, B. S. Wang, S. Lin, P. Tong, W. J. Lu, L. Zhang, W. H. Song, and Y. P. Sun, *J. Appl. Phys.* **111**, 043905 (2012).

¹⁰C. Wang, L. H. Chu, Q. R. Yao, Y. Sun, M. M. Wu, L. Ding, J. Yan, Y. Y. Na, W. H. Tang, G. N. Li, Q. Z. Huang, and J. W. Lynn, *Phys. Rev. B* **85**, 220103(R) (2012).

¹¹K. Takenaka, M. Ichigo, T. Hamada, A. Ozawa, T. Shibayama, T. Inagaki, and K. Asano, *Sci. Technol. Adv. Mater.* **15**, 015009 (2014).

¹²I. Yamada, K. Tsuchida, K. Ohgushi, N. Hayashi, J. G. Kim, N. Tsuji, R. Takahashi, M. Matsushita, N. Nishiyama, T. Inoue, T. Irifune, K. Kato, M. Takata, and M. Takano, *Angew. Chem., Int. Ed.* **50**, 6579 (2011).

¹³M. Azuma, W. T. Chen, H. Seki, M. Czapski, S. Olga, K. Oka, M. Mizumaki, T. Watanuki, N. Ishimatsu, N. Kawamura, S. Ishiwata, M. G. Tucker, Y. Shimakawa, and J. P. Attfield, *Nat. Commun.* **2**, 347 (2011).

- ¹⁴K. Oka, K. Nabetani, C. Sakaguchi, H. Seki, M. Czapski, Y. Shimakawa, and M. Azuma, *Appl. Phys. Lett.* **103**, 061909 (2013).
- ¹⁵R. J. Huang, Y. Y. Liu, W. Fan, J. Tan, F. R. Xiao, L. H. Qian, and L. F. Li, *J. Am. Chem. Soc.* **135**, 11469 (2013).
- ¹⁶Y. Y. Zhao, F. X. Hu, L. F. Bao, J. Wang, H. Wu, Q. Z. Huang, R. R. Wu, Y. Liu, F. R. Shen, H. Kuang, M. Zhang, W. L. Zuo, X. Q. Zheng, J. R. Sun, and B. G. Shen, *J. Am. Chem. Soc.* **137**, 1746 (2015).
- ¹⁷K. Takenaka and M. Ichigo, *Compos. Sci. Technol.* **104**, 47 (2014).
- ¹⁸K. Nabetani, Y. Muramatsu, K. Oka, K. Nakano, H. Hojo, M. Mizumaki, A. Agui, Y. Higo, N. Hayashi, M. Takano, and M. Azuma, *Appl. Phys. Lett.* **106**, 061912 (2015).
- ¹⁹L. Ding, C. Wang, Y. Y. Na, L. H. Chu, and J. Yan, *Scr. Mater.* **65**, 687 (2011).
- ²⁰K. Takenaka, T. Hamada, D. Kasugai, and N. Sugimoto, *J. Appl. Phys.* **112**, 083517 (2012).
- ²¹J. Yan, Y. Sun, C. Wang, L. H. Chu, Z. X. Shi, S. H. Deng, K. W. Shi, and H. Q. Lu, *Scr. Mater.* **84–85**, 19 (2014).
- ²²K. Takenaka, K. Asano, M. Misawa, and H. Takagi, *Appl. Phys. Lett.* **92**, 011927 (2008).
- ²³T. Hamada and K. Takenaka, *J. Appl. Phys.* **109**, 07E309 (2011).
- ²⁴Because the present analysis cannot provide information about the vertical direction, a nitride grain might be present, embedded shallowly in the 20 μm -outside point in Fig. 2(a), at which the molar ratio differs from that of the copper matrix (Table III).
- ²⁵E. O. Chi, W. S. Kim, and N. H. Hur, *Solid State Commun.* **120**, 307 (2001).
- ²⁶K. Takenaka, A. Ozawa, T. Shibayama, N. Kaneko, T. Oe, and C. Urano, *Appl. Phys. Lett.* **98**, 022103 (2011).
- ²⁷P. Tong, B. S. Wang, and Y. P. Sun, *Chin. Phys. B* **22**, 067501 (2013).
- ²⁸T. A. Hahn, *Thermal Expansion of Metal Matrix Composites, in Metal Matrix Composites: Mechanisms and Properties* (Academic Press, 1991), pp. 329–355.
- ²⁹P. Sebo and P. Stefanik, *Int. J. Mater. Prod. Technol.* **18**, 141 (2003).
- ³⁰Y. Nakamura, K. Takenaka, A. Kishimoto, and H. Takagi, *J. Am. Ceram. Soc.* **92**, 2999 (2009).
- ³¹H. L. Duan and B. L. Karihaloo, *J. Mech. Phys. Solids* **55**, 1036 (2007).
- ³²R. J. Huang, Z. X. Wu, H. H. Yang, Z. Chen, X. X. Chu, and L. F. Li, *Cryogenics* **50**, 750 (2010).
- ³³Z. W. Xue, L. D. Wang, Z. Liu, and W. D. Fei, *Scr. Mater.* **62**, 867 (2010).
- ³⁴J. E. Trujillo, J. W. Kim, E. H. Lan, S. Sharratt, Y. S. Ju, and B. Dunn, *J. Electron. Mater.* **41**, 1020 (2012).
- ³⁵A. Matsumoto, K. Kobayashi, T. Nishio, and K. Ozaki, *Mater. Sci. Forum* **426–432**, 2279 (2003).
- ³⁶D. K. Balch and D. C. Dunand, *Metall. Mater. Trans. A* **35A**, 1159 (2004).
- ³⁷Q. Q. Liu, J. Yang, X. N. Cheng, G. S. Liang, and X. J. Sun, *Ceram. Int.* **38**, 541 (2012).
- ³⁸A. Sakamoto, T. Matano, and H. Takeuchi, *IEICE Trans. Electron.* **E83C**, 1441 (2000); available at http://apps.webofknowledge.com/full_record.do?locale=en_US&errorKey=&qid=6&log_event=yes&viewType=fullRecord&SID=R1Ev11ekKrrdFh3v2vB&product=WOS&doc=1&search_mode=CitedFullRecord&colName=WOS.